



MhpA Is a Hydroxylase Catalyzing the Initial Reaction of 3-(3-Hydroxyphenyl)Propionate Catabolism in *Escherichia coli* K-12

Ying Xu,^{a,b} Ning-Yi Zhou^{a,b}

^aState Key Laboratory of Microbial Metabolism & School of Life Sciences and Biotechnology, Shanghai Jiao Tong University, Shanghai, China

^bJoint International Research Laboratory of Metabolic and Developmental Sciences, Shanghai Jiao Tong University, Shanghai, China

ABSTRACT *Escherichia coli* K-12 and some other strains have been reported to be capable of utilizing 3-(3-hydroxyphenyl)propionate (3HPP), one of the phenylpropanoids from lignin. Although other enzymes involved in 3HPP catabolism and their corresponding genes from its degraders have been identified, 3HPP 2-hydroxylase, catalyzing the first step of its catabolism, has yet to be functionally identified at biochemical and genetic levels. In this study, we investigated the function and characteristics of MhpA from *E. coli* strain K-12 (MhpA_{K-12}). Gene deletion and complementation showed that *mhpA* was vital for its growth on 3HPP, but the *mhpA* deletion strain was still able to grow on 3-(2,3-dihydroxyphenyl)propionate (DHPP), the hydroxylation product transformed from 3HPP by MhpA_{K-12}. MhpA_{K-12} was overexpressed and purified, and it was likely a polymer and tightly bound with an approximately equal number of moles of FAD. Using NADH or NADPH as a cofactor, purified MhpA_{K-12} catalyzed the conversion of 3HPP to DHPP at a similar efficiency. The conversion from 3HPP to DHPP by purified MhpA_{K-12} was confirmed using high-performance liquid chromatography and liquid chromatography-mass spectrometry. Bioinformatics analysis indicated that MhpA_{K-12} and its putative homologues belonged to taxa that were phylogenetically distant from functionally identified FAD-containing monooxygenases (hydroxylases). Interestingly, MhpA_{K-12} has approximately an extra 150 residues at its C terminus in comparison to its close homologues, but its truncated versions MhpA_{K-12}⁴⁰⁰ and MhpA_{K-12}⁴⁸⁰ (with 154 and 74 residues deleted from the C terminus, respectively) both lost their activities. Thus, MhpA_{K-12} has been confirmed to be a 3HPP 2-hydroxylase catalyzing the conversion of 3HPP to DHPP, the initial reaction of 3HPP degradation.

IMPORTANCE Phenylpropionate and its hydroxylated derivatives resulted from lignin degradation ubiquitously exist on the Earth. A number of bacterial strains have the ability to grow on 3HPP, one of the above derivatives. The hydroxylation was thought to be the initial and vital step for its aerobic catabolism via the *meta* pathway. The significance of our research is the functional identification and characterization of the purified 3HPP 2-hydroxylase MhpA from *Escherichia coli* K-12 at biochemical and genetic levels, since this enzyme has not previously been expressed from its encoding gene, purified, and characterized in any bacteria. It will not only fill a gap in our understanding of 3HPP 2-hydroxylase and its corresponding gene for the critical step in microbial 3HPP catabolism but also provide another example of the diversity of microbial degradation of plant-derived phenylpropionate and its hydroxylated derivatives.

KEYWORDS 3-(3-hydroxyphenyl)propionate, 3-(2,3-dihydroxyphenyl)propionate, phenylpropionate, catabolism, MhpA, 2-hydroxylase, *Escherichia coli* K-12

Microbes play a vital role in the carbon cycle of phenylalkanoic acids and their hydroxylated derivatives ubiquitously exist, which is largely resulted from the catabolism of lignin and other plant-derived phenylpropanoids and flavonoids on the

Citation Xu Y, Zhou N-Y. 2020. MhpA is a hydroxylase catalyzing the initial reaction of 3-(3-hydroxyphenyl)propionate catabolism in *Escherichia coli* K-12. *Appl Environ Microbiol* 86:e02385-19. <https://doi.org/10.1128/AEM.02385-19>.

Editor Maia Kivisaar, University of Tartu

Copyright © 2020 American Society for Microbiology. All Rights Reserved.

Address correspondence to Ning-Yi Zhou, ningyi.zhou@sjtu.edu.cn.

Received 18 October 2019

Accepted 4 December 2019

Accepted manuscript posted online 6 December 2019

Published 3 February 2020

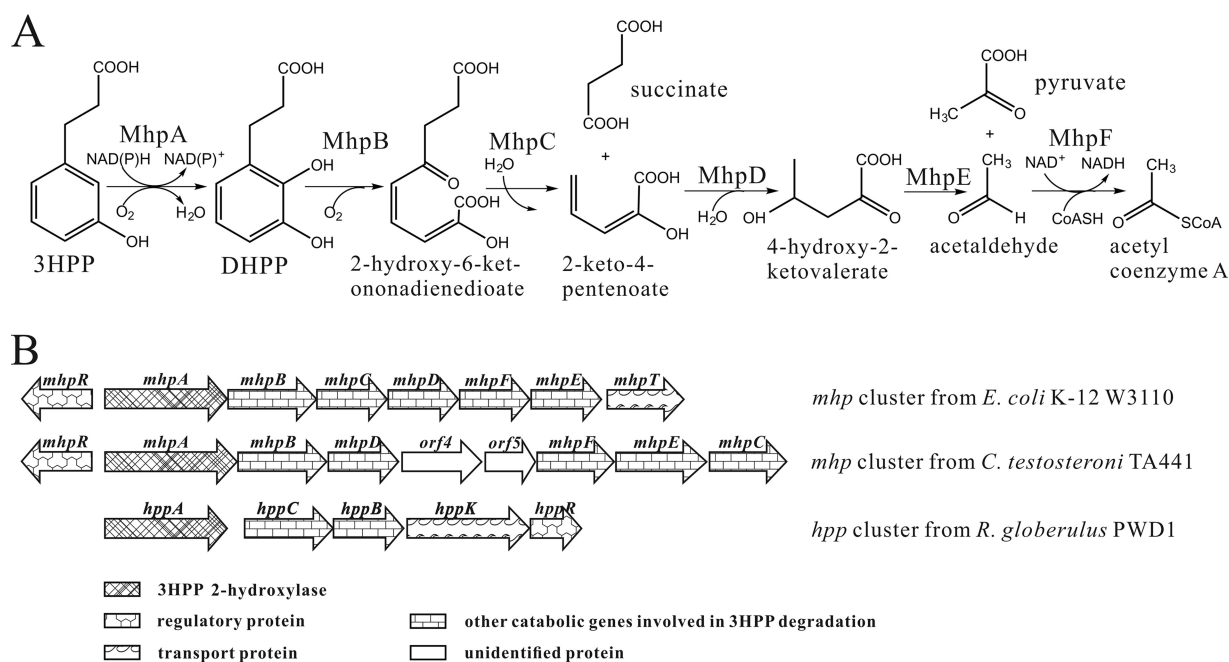


FIG 1 (A) Proposed pathway for 3HPP degradation by *E. coli* K-12 via the *meta* pathway, together with the catabolic reactions catalyzed by the *mhp* gene products *in vivo*. (B) Comparison of the genetic organization of 3HPP catabolic clusters from three 3HPP utilizers. As shown in panel A, *mhpB* encoded 2,3-dihydroxyphenylpropionate 1,2-dioxygenase (21), *MhpR* was a regulatory protein induced by 3HPP (22), and *mhpT* encoded an energy-dependent 3HPP transporter (1). In panel B, the arrows indicate the size and direction of transcription of each gene or open reading frame. Three functionally identified catabolic gene clusters, including *mhpA* and its homologues, for the entire 3HPP degradation pathway are present in the three identified 3HPP utilizers (7, 8, 20), respectively.

Earth (1–5). It has already been reported that phenylpropionate and its hydroxylated derivatives, an important group of phenylpropanoid compounds, were degraded by a number of bacterial strains in previous studies (3, 6–10). Particularly, strains from *Escherichia coli* (including strain K-12) (3), *Rhodococcus globerulus* (strain PWD1) (7), and *Comamonas testosteroni* (strain TA441) (8) could utilize 3-(3-hydroxyphenyl)propionate (3HPP), a key member of the phenylpropanoids, for their growth. As described below, a single hydroxylation has been proved to be the initial step for the aerobic degradation of various 3-hydroxyaromatic acids by different strains. Enzyme 3-hydroxybenzoate 6-hydroxylase catalyzed the reaction of 3-hydroxybenzoate (3HBA) to gentisate in *Polaromonas naphthalenivorans* CJ2 (11), *Klebsiella pneumoniae* M5a1 (4), *Pseudomonas alcaligenes* NCIMB 9867 (12), and *Rhodococcus* sp. strain NCIMB 12038 (13), whereas 3-hydroxybenzoate 4-hydroxylase catalyzed the conversion of 3HBA to 3,4-dihydroxybenzoate in *Comamonas testosteroni* (14, 15) and *Aspergillus niger* (16). For the initial reaction of catabolism of 3-hydroxyphenylacetate (3HPA), its hydroxylation was catalyzed by 3HPA 4-hydroxylase to 3,4-dihydroxyphenylacetate in various *E. coli* strains excluding strain K-12 (17), while 3-hydroxyphenylacetate 6-hydroxylase catalyzed the hydroxylation of 3HPA to 2,5-dihydroxyphenylacetate in *Flavobacterium* sp. strain JS-7 (18) and *Aspergillus nidulans* (19). Finally, for the 3HPP catabolism, it was proved via 3-(2,3-dihydroxyphenyl)propionate (DHPP) for the subsequent ring-cleavage reaction in *E. coli* K-12 (3, 20), *Rhodococcus globerulus* PWD1 (7), and *Comamonas testosteroni* TA441 (8), indicating that the hydroxylation catalyzed by 3HPP 2-hydroxylase (3HPP 2-monooxygenase) was also the initial and vital step for aerobic degradation of 3HPP (Fig. 1A). The specific activity of 3HPP 2-hydroxylase was assayed directly by crude cell extracts of wild-type *E. coli* K-12 using NADH as the cofactor (3) and indirectly with an oxygen electrode by intact washed cells of *E. coli* K-12 (10). The product DHPP resulting from cell extract with a 2,2'-bipyridyl-inhibited reaction was identified by using thin-layer chromatography (3). However, unlike enzymes for all pathways for 3HBA and 3HPA degradation, the hydroxylase catalyzing the initial reaction for 3HPP catabolism has not been purified and characterized.

During a previous study on the 3HPP degradation by *E. coli* K-12, the expression of a 9.8-kb fragment containing *mhpRABCD FE* (accession number D86239, Fig. 1B) from strain K-12 conferred a heterologous host the ability of growing on 3HPP, suggesting that the *mhp* cluster alone was adequate for the entire 3HPP catabolism to central intermediates (20). Among the *mhp* genes, *mhpB* encoded 2,3-dihydroxyphenylpropionate 1,2-dioxygenase (21), *mhpR* was functionally identified to encode a regulatory protein required for *mhp* genes transcription, which was induced by 3HPP (22), and *mhpT* encoded an energy-dependent 3HPP transporter and was necessary for the growth of strain K-12 on 3HPP under basic conditions (1). Although MhpA from strain K-12 (MhpA_{K-12}; accession number BAA13052) was annotated as a 3HPP 2-hydroxylase (20), its function is yet to be identified. In another 3HPP degrader, *Rhodococcus globerulus* PWD1, *hpp* genes (*hppA* and *hppCBKR*) (accession number U89712), homologous to the aforementioned *mhp* genes from strain K-12, were also proposed to be involved in 3HPP degradation (7). However, no 3HPP 2-hydroxylase activity was detected from the cell extracts of the 3HPP-grown strain PWD1 with NADH or NADPH as a cofactor, and no identification of 3HPP 2-hydroxylase gene (*hppA*) was reported either (7). On the other hand, the 3HPP catabolism by *Comamonas testosteroni* TA441 was thought to be encoded by another *mhp* gene cluster (accession number ABO24335) (8). MhpA_{TA441} (accession number BAA82878) was similar to its homologue MhpA_{K-12} and HppA_{PWD1} (accession number AAB81312) (8), but there was no report for its hydroxylase activity (8). The authors working on strain PWD1 proposed that the failure to functionally identify this hydroxylase involved in the initial reaction of 3HPP catabolism in multiple cases was probably due to its special and unknown nature (7).

So far, all the enzymes involved in the catabolism of 3HPP have been functionally identified, except for the one catalyzing the initial reaction. The lack of functional identification and characterization of 3HPP 2-hydroxylase has hampered the recognition of its catabolic role. This study, therefore, reports the functional expression, purification, and characterization of MhpA_{K-12}, confirming its identity as a 3HPP 2-hydroxylase catalyzing the hydroxylation of 3HPP to form DHPP in 3HPP degradation. This will fill a gap in our understanding of 3HPP 2-hydroxylase and its corresponding genes for the initial and critical step in microbial catabolism of phenylpropionate and its hydroxylated derivatives at biochemical and genetic levels.

RESULTS

***mhpA* is vital for 3HPP catabolism in *E. coli* K-12.** *mhpA* was deleted and complemented to identify its possible role in 3HPP degradation in *E. coli* K-12 W3110. Wild-type strain W3110, mutant strain W3110 $\Delta mhpA$, and complemented strain W3110 $\Delta mhpA$ (pRK415-*mhpA*) grew in minimal medium (MM) with 2 mM 3HPP or DHPP at 37°C, respectively. Growth data are shown in semilog plots (Fig. 2), and the maximum specific growth rates (μ_{\max} h⁻¹) of the above strains were determined (Table 1). Mutant strain W3110 $\Delta mhpA$ completely lost the ability to utilize 3HPP for growth, but the complemented strain W3110 $\Delta mhpA$ (pRK415-*mhpA*) regained the growth ability on 3HPP with a growth rate similar to that of the wild-type strain W3110 (Fig. 2 and Table 1). In contrast, when DHPP was used as a substrate, the absence of *mhpA* had no effect on the growth of mutant strain W3110 $\Delta mhpA$. The mutant exhibited a growth rate similar to those of wild-type strain W3110 and complemented strain W3110 $\Delta mhpA$ (pRK415-*mhpA*). Nonetheless, the maximum specific growth rates of strains W3110 and W3110 $\Delta mhpA$ (pRK415-*mhpA*) growing on 3HPP were approximately two times higher than those growing on DHPP.

Overexpression and purification of MhpA_{K-12}. *mhpA* was overexpressed in strain *E. coli* Rosetta(DE3)pLysS(pET-28a-*mhpA*) as a C terminus His-tagged fusion protein. SDS-PAGE analysis indicated that the purified MhpA_{K-12} with a single polypeptide was approximately 61.0 kDa in molecular weight (Fig. 3C). Compared to the protein standards, the molecular mass of MhpA_{K-12} was about 669 kDa as deduced from detection using a BioLogic DuoFlow system (Bio-Rad) equipped with column Superdex

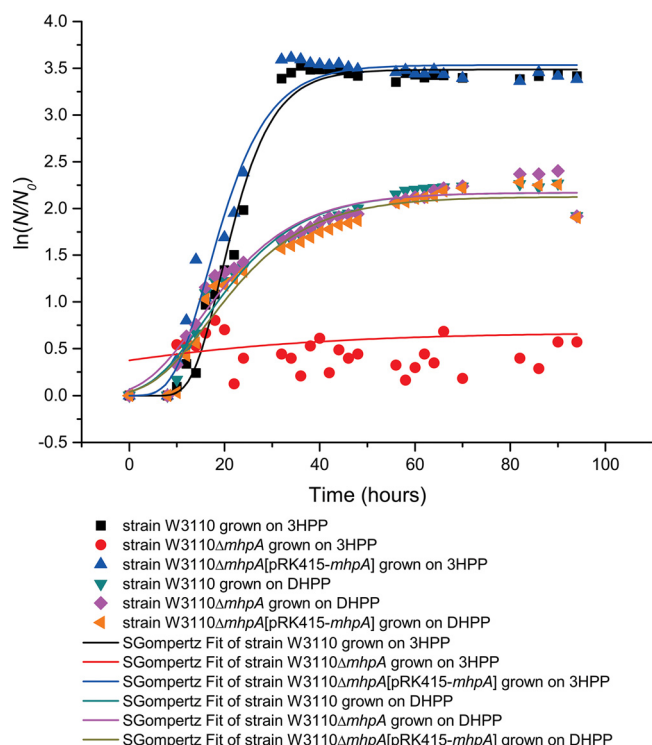


FIG 2 Growth curves of *E. coli* K-12 W3110 and its *mhpA* deletion and complementary strains on 3HPP and DHPP. Strains were grown in MM [containing 6 mM (NH₄)₂SO₄ (pH 7.2)] (1) with 2 mM 3HPP and DHPP on a Bioscreen C MBR at 37°C, respectively. *N*₀, initial number of cells; *N*, number of cells. The growth curves were fitted by the modified Gompertz equation (49) with OriginPro (version 9.1) software, and all points represent mean values of three parallel experiments. The maximum specific growth rates (μ_{max} h⁻¹) were also calculated based on mean values from three parallel experiments (Table 1).

200 10/300 GL (GE Healthcare) (see Fig. S1 in the supplemental material), suggesting that MhpA_{K-12} is likely a polymer.

MhpA_{K-12} catalyzes the hydroxylation of 3HPP to DHPP. The purified MhpA_{K-12} had the ability to catalyze the hydroxylation of 3HPP to DHPP. A time course assay of 3HPP hydroxylation catalyzed by purified MhpA_{K-12} (Fig. 4) was monitored by high-performance liquid chromatography (HPLC). As shown in Fig. 4, the substrate 3HPP gradually reduced and the product DHPP gradually increased in the presence of NADH. The consumption of 3HPP (45.0 μM) was almost equal to the accumulation of DHPP (44.5 μM) after 14 min of incubation, indicating a stoichiometry conversion of 3HPP to DHPP. Samples incubated for 4 min in the time course were withdrawn to confirm the identities of the substrate 3HPP and the product DHPP by liquid chromatography-mass spectrometry (LC-MS). The authentic 3HPP (*m/z* = 165.0553) and DHPP (*m/z* = 181.0486) both contained the stable deprotonated ion of [M-H]⁻ in mass spectrum (Fig. 5A and B), and the product converted from 3HPP (*m/z* = 165.0548) by MhpA_{K-12} was confirmed as DHPP (*m/z* = 181.0503) (Fig. 5C).

TABLE 1 Maximum specific growth rates of *E. coli* K-12 W3110 and its two variants on 3HPP and DHPP

<i>E. coli</i> strain	Maximum specific growth rate (μ_{max} h ⁻¹)	
	3HPP (2 mM)	DHPP (2 mM)
K-12 W3110	0.213	0.071
K-12 W3110 Δ <i>mhpA</i>	0.008	0.069
K-12 W3110 Δ <i>mhpA</i> (pRK415- <i>mhpA</i>)	0.182	0.066

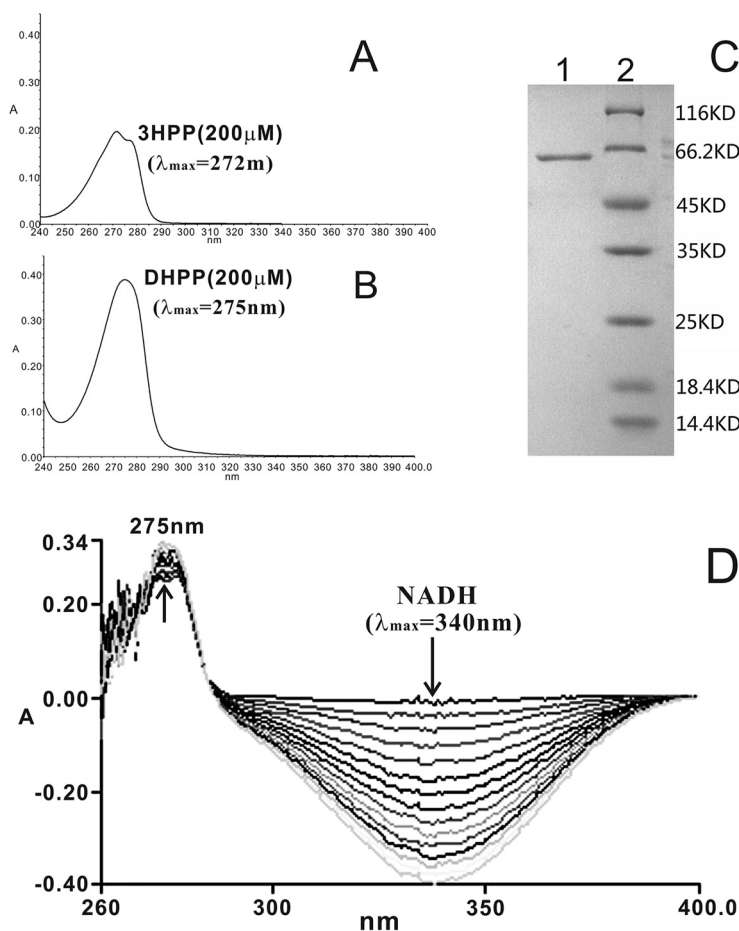


FIG 3 Spectrophotometric scan of authentic 3HPP (A) and DHPP (B), SDS-PAGE of purified MhpA_{K-12} (C), spectrophotometric changes in the hydroxylation of 3HPP by purified MhpA_{K-12} with NADH as a cofactor (D). (A and B) The concentrations of 3HPP and DHPP standards were both 0.2 mM in the sample cuvettes, and 50 mM phosphate buffer (pH 7.4) was used as the negative control. (C) Lane 1, purified MhpA_{K-12} (~61.0 kDa in molecular weight); lane 2, molecular mass standards (molecular masses are indicated on the right). (D) The 0.5-ml reaction mixtures in the cuvettes contained 50 mM phosphate buffer (pH 7.4), 200 μM NADH or NADPH, 10 μM FAD, and 180 μg of purified MhpA_{K-12} proteins. All assays were initiated with 0.3 mM 3HPP added to the sample cuvettes. The UV spectra at 220 to 400 nm were measured at regular time intervals (30 s) by a Lambda 25 UV/VIS spectrometer (Perkin-Elmer). The arrows indicate the direction of spectral changes at 275 and 340 nm.

Biochemical properties of MhpA_{K-12}. The maximum absorbance of authentic 3HPP and DHPP appeared at 272 and 275 nm, respectively (Fig. 3A and B). The slightly higher absorbance for DHPP compared to 3HPP at the same concentration (Fig. 3A and B) indicates that the molar extinction coefficient of DHPP is a bit larger than that of 3HPP. This makes possible to observe the conversion of 3HPP to DHPP, although the hydroxylation activity determination was based on the NADH consumption. When purified MhpA_{K-12} was used to determine the enzyme activity, NADH was consumed in the sample cuvette, and negative absorbance at 340 nm appeared, as shown in Fig. 3D. Meanwhile, the absorption peak of 275 nm also slightly rose due to the consumption of 3HPP and the accumulation of DHPP being largely overlapped and similar molar extinction coefficients between the substrate and the product (Fig. 3D). As shown in Table 2, the purified MhpA_{K-12} contained the specific activities of 0.94 ± 0.06 and 0.61 ± 0.08 U mg⁻¹ with NADH and NADPH as cofactors, respectively. This indicated that NADH was a more suitable cofactor than NADPH for MhpA_{K-12}-catalyzed 3HPP hydroxylation. The kinetic assays also revealed that the K_m (381.10 ± 72.41 μM for NADH and 436.70 ± 67.40 μM for NADPH) and k_{cat} (41.47 ± 5.49 min⁻¹ for NADH and

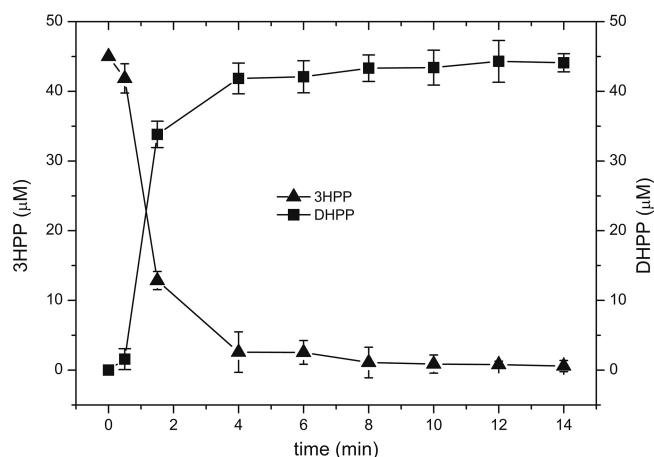


FIG 4 Time course assay of 3HPP hydroxylation catalyzed by purified MhpA_{K-12}. The system was carried out using 20 ml of 50 mM phosphate buffer (pH 7.4) containing 45 μM 3HPP, 200 μM NADH, 10 μM FAD, and 215 μg of purified MhpA_{K-12}. Samples were withdrawn at the indicated time points from this system and treated immediately as described in the text. The consumption of 3HPP and the accumulation of DHPP were quantified by HPLC. All points represent the mean values of triplicate trials, with error bars denoting standard deviations.

44.14 ± 2.80 min⁻¹ for NADPH values were similar with NADH and NADPH (Table 2). These results proved that the two cofactors have similar affinities for purified MhpA_{K-12}.

MhpA_{K-12} was proposed to contain an FAD domain according to its protein sequence alignment. The light yellow-brown color of purified MhpA_{K-12} proved this bioinformatics prediction. The presence of FAD in purified MhpA_{K-12} was confirmed at

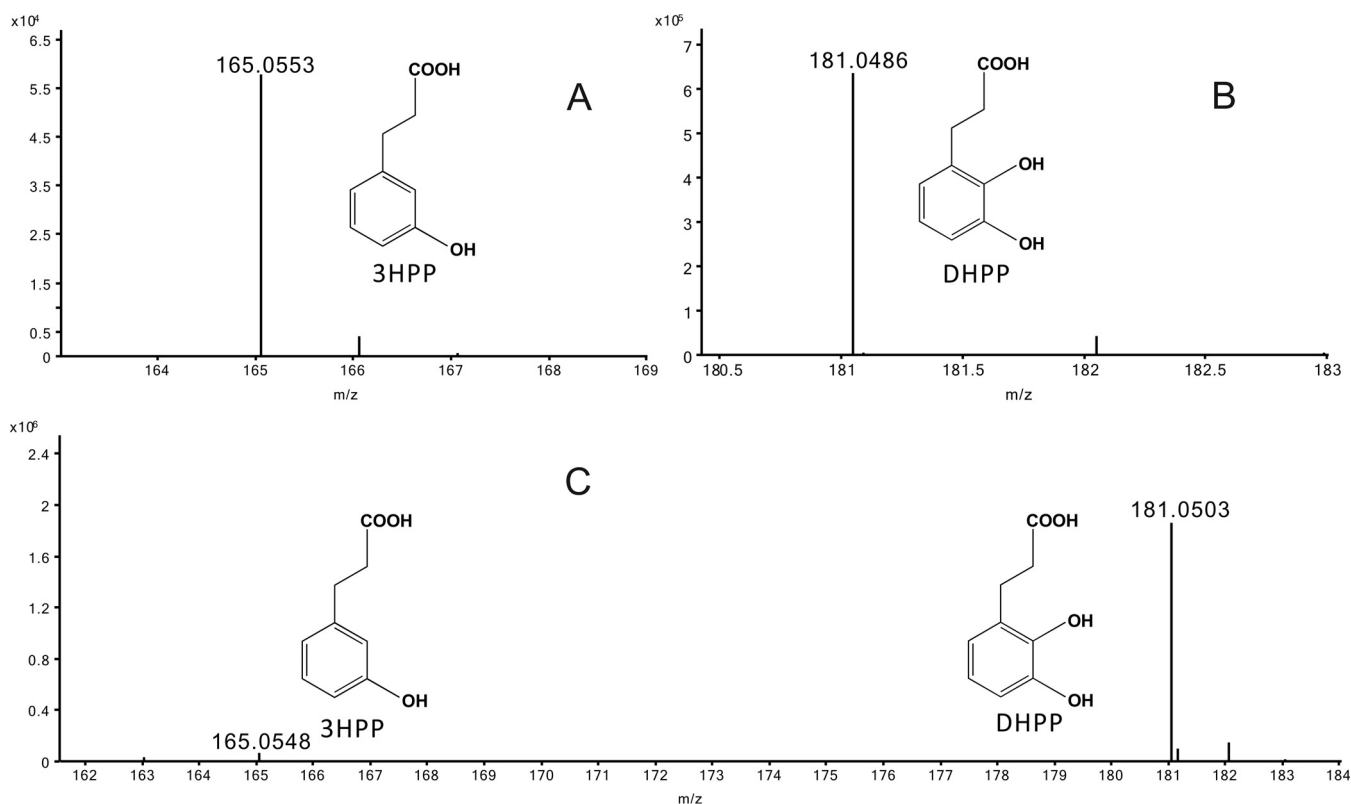


FIG 5 Mass spectra of authentic 3HPP (A), authentic DHPP (B), and the substrate 3HPP and the product DHPP from the hydroxylation catalyzed by MhpA_{K-12}. The standards of 3HPP ($m/z = 165.0553$) (A) and DHPP ($m/z = 181.0486$) (B) both contained the stable deprotonated ion of [M-H]⁻ in the mass spectrum, and the product of 3HPP ($m/z = 165.0548$) was confirmed as DHPP ($m/z = 181.0503$) (C).

TABLE 2 Characteristics of MhpA_{K-12} with NADH and NADPH as cofactors

Cofactor	Mean ± the SEM			
	Sp act (U mg ⁻¹)	K _m (μM)	k _{cat} (min ⁻¹)	k _{cat} /K _m (μM ⁻¹ min ⁻¹)
NADH	0.94 ± 0.06	381.10 ± 72.41	41.47 ± 5.49	0.11 ± 0.08
NADPH	0.61 ± 0.08	436.70 ± 67.40	44.14 ± 2.80	0.10 ± 0.04

445 nm by HPLC with the same retention time (9.61 min) as for the FAD standard. A quantification analysis indicated that 1 mol of purified MhpA_{K-12} was bound with 0.81 mol of FAD, suggesting that approximately equal number of moles of FAD was tightly bound to MhpA_{K-12}.

When the derivatives of 3HPP were used as substrates, MhpA_{K-12} showed no activity in response to phenylpropionic acid, 3-hydroxybenzoate, *cis*-cinnamic acid, *trans*-cinnamic acid, and benzoate and had extremely weak activity in response to 3-hydroxycinnamic acid.

Phylogenetic analysis reveals divergent origins of FAD-containing monooxygenases. MhpA_{K-12} is a single-component enzyme containing the FAD-binding domain. A distance UPGMA (unweighted pair-group method with arithmetic averages) tree was constructed using the MEGA package (version 5.0) to elucidate the phylogenetic relationship between MhpA_{K-12} and the other FAD-containing monooxygenases (hydroxylases) (Fig. 6). The other FAD-containing monooxygenases (hydroxylases) in the phylogenetic tree include (i) putative 3HPP 2-hydroxylases (accession numbers [AAZ59652](#), [BAA82878](#), [ABB81312](#), [AEI82814](#), [AGI74442](#), [CDO14979](#), [AUR37237](#),

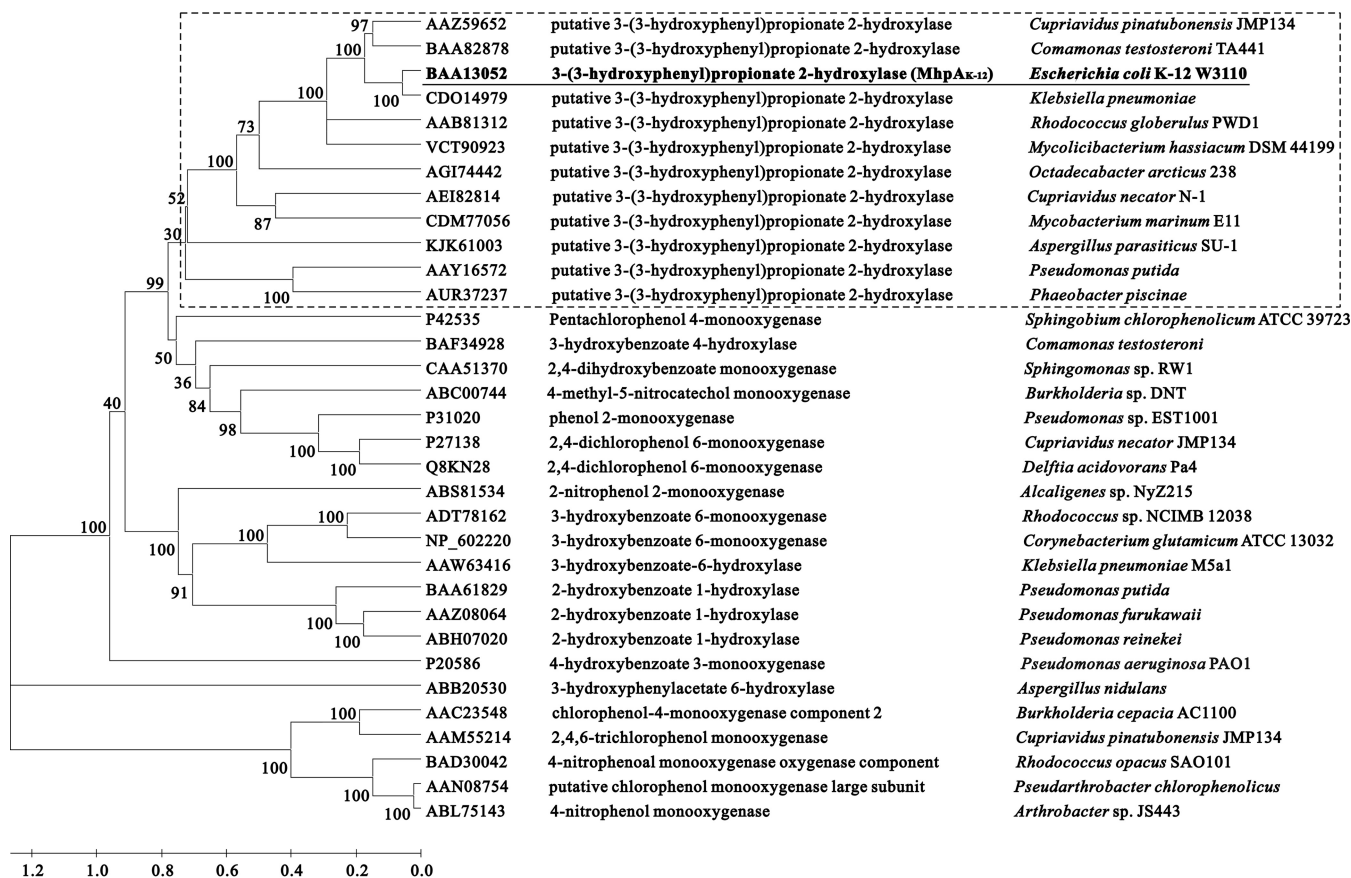


FIG 6 Phylogenetic relationships of MhpA_{K-12} and other FAD-containing monooxygenases (hydroxylases). All protein sequences were aligned by Clustal W, and the distance UPGMA tree was created by the MEGA package (v5.0); bootstrap confidence limits are expressed as percentages and indicated at the nodes. The group of 3HPP 2-hydroxylases belonged to phylogenetically distant taxa and were distantly related to 2HBA, 3HBA, 3HPA, and nitro- or chloro-aromatic monooxygenases (hydroxylases).



FIG 7 MhpA_{K-12} and its C-terminal truncated proteins MhpA_{K-12}⁴⁰⁰ and MhpA_{K-12}⁴⁸⁰. There was a FAD-binding domain spanning 400 amino acid residues from the N terminus of MhpA_{K-12}. MhpA_{K-12}⁴⁰⁰, MhpA_{K-12} with a 154-residue deletion from the C terminus; MhpA_{K-12}⁴⁸⁰, MhpA_{K-12} with a 74-residue deletion from the C terminus. Only MhpA_{K-12} possessed 3HPP 2-hydroxylase activity, and the two truncated mutants lost enzyme activity.

CDM77056, KJK61003, VCT90923, and AAY16572) from either bacteria or fungi (7–9, 23–26), (ii) functionally identified FAD-binding monooxygenases (hydroxylases), such as 3-hydroxyaromatic acid hydroxylases (accession numbers AAW63416, ADT78162, NP_602220, BAF34928, ABB20530) (4, 13, 14, 19, 27–29), (iii) nitro- or chloro-aromatic hydroxylases or monooxygenases (accession numbers P27138, ABS81534, P42535, AAM55214, BAD30042, and AAC23548) (30–36), etc. The results indicated that MhpA_{K-12} in this study was only most closely related to the putative 3HPP 2-hydroxylases. The group of 3HPP 2-hydroxylases was distantly related with 2HBA, 3HBA, 3HPA, and nitro- and chloro-aromatic monooxygenases (hydroxylases), which belong to a phylogenetically distant multiorigin taxa. It suggested that the group of 3HPP 2-hydroxylases had a divergent origin with the other FAD-containing monooxygenases (hydroxylases).

Truncated MhpA_{K-12} mutants exhibited no 3HPP 2-hydroxylase activity. Despite the fact that all 3-hydroxyaromatic acid hydroxylases contained FAD-binding domain in the N terminus, they vary significantly in protein size. Apart from MhpA_{K-12} containing 554 amino acids in this study, the other functionally identified one-component 3-hydroxyaromatic acid hydroxylases, namely, 3HBA 6-hydroxylase MhbM (accession number AAW63416) from *Klebsiella pneumoniae* (4), NarX (accession number ADT78162) from *Rhodococcus* sp. strain NCIMB 12038 (13), Ncgl2923 (accession number NP_602220) from *Corynebacterium glutamicum* (27, 28), 3HBA 4-hydroxylase MobA (accession number BAF34928) from *Comamonas testosteroni* KH122-3s (14, 29), and 3HPA 6-hydroxylase PhacB (accession number ABB20530) from the fungus *Aspergillus nidulans* (19), contained 397, 400, 442, 569, and 517 residues, respectively.

Interestingly, upon comparing the amino acid sequence of MhpA_{K-12} to its homologues from the NCBI database and the five identified 3-hydroxyaromatic acid hydroxylases listed above, we found that they all have FAD-binding domain in the N terminus. The 154 residues in the C terminus of MhpA_{K-12} have no similarity to the known domains of enzymes, so these 154 residues seem to be superfluous. However, MhpA_{K-12}⁴⁰⁰ (with 154 residues deleted from the C terminus) and MhpA_{K-12}⁴⁸⁰ (with a 74-residue deletion) both virtually lost the ability to catalyze the hydroxylation of 3HPP to DHPP (Fig. 7). This indicated that the 154 amino acid residues in the C terminus of MhpA_{K-12} played important roles in its hydroxylation activity.

DISCUSSION

It is well known that phenylpropionate and its hydroxylated derivatives mostly result from lignin degradation, exist broadly on the Earth, and can be degraded by a number of bacterial strains from different genera (3, 6–10), including some 3HPP utilizers (3, 7, 8, 20). Although 3HPP 2-hydroxylase activity was detected directly in the crude cell extracts of wild-type *E. coli* K-12 (3) and indirectly with an oxygen electrode using intact washed cells of *E. coli* K-12 (10) in the 1980s, the purification of this enzyme has not been reported, and there are no appropriate biochemical characterizations of this enzyme. On the other hand, the 3HPP catabolic gene clusters from *E. coli* K-12 (20), *R. globerulus* PWD1 (7), and *C. testosteroni* TA441 (8) (Fig. 1B) were reported in the late 1990s, but no 3HPP 2-hydroxylase was functionally expressed from its encoding gene

in any of aforementioned three clusters. In this study, we have successfully expressed and purified 3HPP 2-hydroxylase from its *E. coli* K-12 encoding gene *mhpA*. Indeed, many other MhpA-like proteins from either bacteria or fungi were also annotated as putative 3HPP 2-hydroxylases in the NCBI database (9, 23–26, 37), indicating the widespread dissemination and importance of 3HPP degraders in the environment.

Although MhpA_{K-12} is relatively closely related to the putative 3HPP 2-hydroxylases in a constructed phylogenetic tree, shown in Fig. 5, their identities vary significantly (ranging from 20 to 80%), indicating the presence of possible multiple evolutionary ancestors. Since the widespread distribution of 3HPP in the environment and the hydroxylation being the initial and vital step for the aerobic degradation of 3-hydroxyaromatic acids, the genes for putative 3HPP 2-hydroxylase and other enzymes in the entire 3HPP degradation pathway are mostly ubiquitous in microbial genomes through natural evolution, as determined from data mining the NCBI database. Furthermore, some putative 3HPP 2-hydroxylases annotated in the NCBI database exhibited low identities with MhpA_{K-12}, such as MhpA proteins from marine bacterium *Mycobacterium marinum* E11 (accession number [CDM77056](#), with 28% identity) and the fungus *Aspergillus parasiticus* SU-1 (accession number [KJK61003](#), with 20% identity), but these two strains also contained other genes encoding putative enzymes for the entire 3HPP degradation pathway. This research indicated that *mhpA*-like genes in strains from terrestrial and marine habitats had different origins, as did bacteria and fungi. On the other hand, HppA_{PWD1} from strain PWD1 (7), MhpA_{JMP134} (accession number [AAZ59652](#)) from *Cupriavidus pinatubonensis* (originally *Cupriavidus necator*) JMP134 (9), and MhpA_{TA441} from strain TA441 (8) showed moderate identities (56.7, 55.1, and 47.9%, respectively) to MhpA_{K-12}. In contrast, MhpA_{Kp} (accession number [CDO14979](#)) from *Klebsiella pneumoniae* (25) showed high identity (79.3%) with MhpA_{K-12}, reflecting their close taxonomic relationship. The widespread presence of 3HPP catabolic clusters in phylogenetically divergent species particularly shows that their important roles in the carbon cycle of intermediates resulted from lignin degradation.

Although the 3-hydroxyaromatic acids 3HPP, 3HBA, and 3HPA are structural analogues, their hydroxylases involved in their catabolism have evident differences in protein sequence, component number, and substrate specificity. Despite being a one-component hydroxylase, MhpA_{K-12} in this study is distantly related to other functionally identified one-component hydroxylases (Fig. 6), exhibiting low identities (no more than 20%) to 3HBA 6-hydroxylases MhbM (4), NarX (13), Ncgl2923 (27, 28), 3HBA 4-hydroxylase MobA (14, 29), and 3HPA 6-hydroxylase PhacB (19). In contrast to these enzymes, MhaAB from *P. putida* is a two-component 3HPA 6-hydroxylase (38). In addition, previous reports proved that studied 3-hydroxyaromatic acid hydroxylases possess narrow substrate specificity (11, 13, 27–29), and MhpA_{K-12} in the present study is no exception. This indicates that although 3-hydroxyaromatic acids all contained aromatic ring and hydroxyl group substituted at the same position, the different carboxylic acid groups require specific enzymes with different spatial structures to make individual hydroxylation happen. Although the crystal structure of several 3-hydroxyaromatic acids and other FAD-binding hydroxylases have been resolved (14, 39–42), the simulation structure of MhpA_{K-12} could not be established. This is because all known model templates of aforementioned enzymes in SWISS-MODEL (<https://www.swissmodel.expasy.org/>), including PnpA (*p*-nitrophenol 4-monooxygenase) from *Pseudomonas putida* DLL-E4 (42), MobA (3HBA 4-hydroxylase) from *C. testosteroni* (14, 40), and 2-hydroxybiphenyl 3-monooxygenase from *Pseudomonas azelaica* (43), showed very low identities (no more than 20%) with MhpA_{K-12}. The spatial structure of MhpA_{K-12} and the role of those ~150 extra but critical residues in the C terminus will be thoroughly elucidated by the crystallographic structural analysis in our future investigations.

MATERIALS AND METHODS

Strains, plasmids, primers, media, chemicals, and general growth conditions. All strains and plasmids are shown in Table 3, and all primers are listed in Table 4. The substrates 3-(3-hydroxy-

TABLE 3 Bacterial strains and plasmids used in this study

Strain or plasmid	Relevant characteristics	Reference or source
<i>E. coli</i> strains		
DH5 α	<i>supE44 lacU169(φ80lacZΔM15) hsdR17 recA1 endA1 gyrA96 Δthi relA1</i>	Gibco, BRL
Rosetta(DE3)pLysS	F ⁻ <i>ompT hsdS_B (r_B m_B) gal dcm lacY1 (DE3)pLysSRARE² (Cm^r)</i>	Novagen, USA
K-12 W3110	3-(3-Hydroxyphenyl)propionate utilizer; Km ^s Tc ^s	48
K-12 W3110 Δ <i>mhpA</i>	<i>E. coli</i> K-12 W3110 with DNA fragment encoding <i>mhpA</i> deletion	This study
K-12 W3110 Δ <i>mhpA</i> (pRK415- <i>mhpA</i>)	<i>E. coli</i> K-12 W3110 Δ <i>mhpA</i> complemented with <i>mhpA</i>	This study
Plasmids		
pKD46	Temperature-sensitive vector; Ap ^r	47
pRK415	Broad-host-range expression vector (IncQ, RSF1010 replicon); Tc ^r , Ptac, lacI ^q , Tra ⁻ Mob ⁺	52
pRK415- <i>mhpA</i>	PCR fragment containing <i>mhpA</i> inserted into pRK415 at the EcoRI/HindIII restriction sites	This study
pET-28a	Expression vector; Km ^r	Novagen, USA
pET-28a- <i>mhpA</i>	Km ^r ; pET-28a derivative for the expression of <i>mhpA</i>	This study
pET-28a- <i>mhpA</i> ⁴⁰⁰	Km ^r ; pET-28a derivative for the expression of <i>mhpA</i> ⁴⁰⁰ (<i>mhpA</i> being deleted 465 bp from the 3' end)	This study
pET-28a- <i>mhpA</i> ⁴⁸⁰	Km ^r ; pET-28a derivative for the expression of <i>mhpA</i> ⁴⁸⁰ (<i>mhpA</i> being deleted 225 bp from the 3' end)	This study

phenyl)propionate (3HPP) (purity grade, ≥98%) and 3-(2,3-dihydroxyphenyl) propionate (DHPP) (purity grade, ≥97%) were purchased from Amatek Scientific Co., Ltd. (Zhangjiagang, China). Other aromatics were purchased from Sigma-Aldrich Co. (St. Louis, MO). Methanol (Adamas-beta) was purchased from Adamas Reagent, Ltd. (Shanghai, China). High-fidelity DNA polymerase was purchased from Vazyme Biotech Co., Ltd. (Nanjing, China). T4 DNA ligase and all restriction enzymes were purchased from New England Biolabs, Ltd. (Beijing, China). DNA gel extraction and plasmid DNA extraction kits were purchased from Omega Bio-Tek, Inc. (Doraville, GA). *E. coli* strains DH5 α (Gibco, BRL) and Rosetta(DE3)pLysS (Novagen) were used as hosts for the cloning and overexpression experiments, respectively. All *E. coli* strains were grown at 37°C in lysogeny broth (LB) (44, 45) on a rotary shaker (180 rpm) or in MM [containing 6 mM (NH₄)₂SO₄ (pH 7.2)] (1) with 2 mM 3HPP or DHPP on Bioscreen C MBR (Transgalactic, Ltd., Vantaa, Finland). Ampicillin, tetracycline, and kanamycin were used at final concentrations of 100, 20, and 50 μg/ml, respectively, when necessary. Finally, 0.1 mM (final concentration) IPTG (isopropyl-β-D-thiogalactopyranoside) was used as an inducer.

***mhpA* disruption and complementation.** Plasmid DNA was isolated by plasmid DNA extraction kits according to the alkaline lysis method (46). pKD46, a temperature-sensitive vector (47), was introduced into strain W3110 (48) to prepare competent cells. A kanamycin resistance gene was amplified from pKD4 (47) by PCR with the primers *mhpA*-dF and *mhpA*-dR (Table 4), which separately contained 51-bp 5' and 3' homologous arms of *mhpA*. After being sequenced to confirm without mutations by Sangni Biology Technologies Co., Ltd. (Shanghai, China), the PCR fragment was electroporated into competent cells of strain W3110(pKD46) for the deletion of gene *mhpA*, modified as previously described (47). After 1 h of incubation in 1 ml of LB, shocked cells were then spread onto an agar plate with kanamycin to select transformants. Next, strain W3110 Δ*mhpA* resulted after the confirmed transformants were incubated in liquid LB for 2 h at 42°C to eliminate the pKD46. Meanwhile, *mhpA* was amplified with the primer pair *mhpA*1F and *mhpA*1R (Table 4) from the genomic DNA of strain W3110. After being sequenced to confirm without mutation, the PCR product (digested with PstI and EcoRI) was fused to pRK415 (digested with PstI and EcoRI). Then, pRK415-*mhpA* was introduced into strain W3110 Δ*mhpA* for complementation.

Bacterial growth determination on 3HPP and DHPP. The growth on 3HPP or DHPP of strain W3110 and its gene deletion and complementary variants was monitored with an optical density at 600 nm (OD₆₀₀) by using a Bioscreen C MBR. Similar results were obtained in three parallel experi-

TABLE 4 Primers used in this study

Primer	Sequence ^a (5'–3')	Purpose
<i>mhpA</i> -dF	<u><i>atgqcaatacaaacacccctgacatccaqctgctgttaaccatagcgttcagatagaatatcctccttag</i></u>	Forward primer for kanamycin resistance gene with the homologous arm of <i>mhpA</i>
<i>mhpA</i> -dR	<u><i>tcaggctaccttttcacagaaacctcggcatcaggcgggctcagcgtcattgtaggctggagctccttcg</i></u>	Reverse primer for kanamycin resistance gene with the homologous arm of <i>mhpA</i>
<i>mhpA</i> 1F	ccgctgcagatggcaatacaaacacccctga	Forward primer for <i>mhpA</i>
<i>mhpA</i> 1R	cgcgaaattctcaggctaccttttcgacag	Reverse primer for <i>mhpA</i>
<i>mhpA</i> 2F	gaacatgatggcaatacaaacacccct	Forward primer for <i>mhpA</i>
<i>mhpA</i> 2R	gaagaattcggctaccttttcgacagaaa	Reverse primer for <i>mhpA</i> without a stop codon
<i>mhpA</i> 3R	gaagaattcgaatattgctgcatcggt	Reverse primer for <i>mhpA</i> being deleted 465 bp from the 3' end
<i>mhpA</i> 4R	gaagaattcatgaattgcacttccggca	Reverse primer for <i>mhpA</i> being deleted 225 bp from the 3' end

^aThe introduced restriction sites are indicated in boldface, and the homologous arms of *mhpA* are underlined and italic.

ments. The growth data for the above three *E. coli* strains were converted into their corresponding cell numbers to plot their growth curves. The growth curves were fitted using the modified Gompertz equation (49), and all points represent the mean values of three parallel experiments. The maximum specific growth rates (μ_{\max} h⁻¹) were also calculated based on the mean values of three parallel experiments.

Protein expression and purification. *mhpA* (without stop codon), *mhpA*⁴⁰⁰ (with 465 bp deleted from the 3' end), and *mhpA*⁴⁸⁰ (with 225 bp deleted from the 3' end) were amplified using three pairs of primers—*mhpA*2F/*mhpA*2R, *mhpA*2F/*mhpA*3R, and *mhpA*2F/*mhpA*4R (Table 4)—from strain W3110, respectively. The DNA fragments were sequenced without any mutation. The verified PCR products (all digested with PstI and EcoRI) were then fused to pET-28a (digested with PstI and EcoRI) to produce expression plasmids pET-28a-*mhpA*, pET-28a-*mhpA*⁴⁰⁰, and pET-28a-*mhpA*⁴⁸⁰. The cells of strain Rosetta(DE3)pLysS were transformed by standard procedures (46). C-terminal His-tagged MhpA_{K-12}, MhpA_{K-12}⁴⁰⁰, and MhpA_{K-12}⁴⁸⁰ were thus overexpressed in the strains Rosetta(DE3)pLysS(pET-28a-*mhpA*), Rosetta(DE3)pLysS(pET-28a-*mhpA*⁴⁰⁰), and Rosetta(DE3)pLysS(pET-28a-*mhpA*⁴⁸⁰), respectively. These three strains were grown separately in LB with 50 μ g ml⁻¹ kanamycin at 37°C to an OD₆₀₀ of 0.4. The cells were incubated for another 4 h, adding 0.1 mM IPTG at 30°C. The cells were then broken by ultrasonic treatment as previously described (50) and centrifuged at 19,000 \times *g* at 4°C for 50 min, before the cell supernatant was filtered through a 0.45- μ m-pore membrane filter and used for protein purification. According to the manufacturer's instructions, the three His-tagged proteins were purified by using the ÄKTA start system (GE Healthcare) with a 5-ml HisTrap HP column (GE Healthcare), respectively. The elution buffer used in the purification consisted of 50 mM phosphate buffer containing 135 mM NaCl, 10% glycerol, and 250 mM imidazole (pH 7.4). The purified proteins were desalted using HiTrap 5-ml desalting (GE Healthcare) with 50 mM phosphate buffer containing 135 mM NaCl and 10% glycerol (pH 7.4). The purified proteins were then stored at -80°C before being assessed by SDS-PAGE. All of the purification procedures were performed at 4°C, as previously described (51).

Enzyme activity assay. To assay 3HPP hydroxylation to DHPP mediated by 3HPP 2-hydroxylase MhpA_{K-12} and its truncated proteins MhpA_{K-12}⁴⁰⁰ and MhpA_{K-12}⁴⁸⁰, we used reaction mixtures in cuvettes containing 50 mM phosphate buffer (pH 7.4), 200 μ M NADH or NADPH, 10 μ M FAD, and 180 μ g of the purified proteins MhpA_{K-12}, MhpA_{K-12}⁴⁰⁰, or MhpA_{K-12}⁴⁸⁰. All assays were initiated by 0.3 mM 3HPP being added into the sample cuvettes. The UV spectra at 220 to 400 nm were measured at regular time intervals (30 s) by a Lambda 25 UV/VIS spectrometer (Perkin-Elmer, Waltham, MA). The molar extinction coefficients at 340 nm for NADH and NADPH were both 6.22×10^3 M⁻¹ cm⁻¹ (50). One unit (U) of enzyme activity was defined as the amount required for the disappearance of 1 μ mol of NADH or NADPH per min at ambient temperature. Specific activities were defined as units per milligram of protein. All experiments were repeated three times.

Time course assay of 3HPP hydroxylation catalyzed by purified MhpA_{K-12}. A time course assay for the conversion of 3HPP to DHPP was performed by purified MhpA_{K-12}. For the time course assay for the MhpA_{K-12}-catalyzed reaction, the procedure was carried out with 20 ml of 50 mM phosphate buffer (pH 7.4) containing 45 μ M 3HPP, 200 μ M NADH, 10 μ M FAD, and 215 μ g of purified MhpA_{K-12}. At 0.5, 1.5, and 4 min and at regular time intervals (2 min) from 4 to 14 min thereafter, 1-ml samples were also taken, mixed with 1 μ l of HCl immediately, and then extracted with an equal volume of ethyl acetate. All ethyl acetate layers collected by centrifugation were analyzed by HPLC or LC-MS to identify or quantify 3HPP and DHPP. All experiments were repeated three times.

Compound identification using HPLC and LC-MS. To separate and identify 3HPP and DHPP, a Waters e2695 separation module with a 2998 PDA detector and a reverse-phase LP-C₁₈ column (5 μ m, 4.6 \times 250 mm) was used at 30°C. The mobile phase contained solvents A (0.1% acetic acid aqueous solution) and B (methanol). The injection volume was 40 μ l, the flow rate was 1.0 ml min⁻¹, and the detection wavelength was 275 nm. During the monitoring, solvent A started at 70%, increased to 80% from 0 to 17 min, dropped to 70% from 17 to 21 min, and then held at 70% from 21 to 40 min. For this gradient program, the retention times of 3HPP and DHPP were 29.5 and 17.5 min, respectively. Compound identification analysis using an LC-MS system (Surveyor; Thermo Fisher Scientific, San Jose, CA) equipped with a diode array detector and an HILIC amide column (2.1 \times 150 mm, 3 μ m; Welch, China) was performed using the same gradient program and detection wavelength by HPLC, but the injection volume and the flow rate were 10 μ l and 0.2 ml min⁻¹, respectively.

To identify and quantify the FAD in the purified MhpA_{K-12}, we used HPLC at 445 nm, modified as described previously (29). The retention time of the FAD standard was 9.61 min. The calibration curve was calculated by detecting the indicated concentrations of the FAD standard. All experiments were repeated three times.

Molecular weight and aggregation form determination. The molecular weight and the aggregation form of MhpA_{K-12} were determined using SDS-PAGE and the BioLogic DuoFlow system (Bio-Rad) equipped with column Superdex 200 10/300 GL (GE Healthcare), respectively.

Data availability. No new sequence data, protein structures, etc., have been reported in this study. GenBank accession numbers are provided in the text for all mentioned proteins and genes.

SUPPLEMENTAL MATERIAL

Supplemental material is available online only.

SUPPLEMENTAL FILE 1, PDF file, 0.1 MB.

ACKNOWLEDGMENTS

This study is supported by the National Natural Science Foundation of China (grants 31570100, 91951106, and 31670107) and the National Key R&D Program of China (grant 2018YFC0309800).

REFERENCES

- Xu Y, Chen B, Chao H, Zhou NY. 2013. *mhpT* encodes an active transporter involved in 3-(3-hydroxyphenyl)propionate catabolism by *Escherichia coli* K-12. *Appl Environ Microbiol* 79:6362–6368. <https://doi.org/10.1128/AEM.02111-13>.
- Diaz E, Ferrandez A, Prieto MA, Garcia JL. 2001. Biodegradation of aromatic compounds by *Escherichia coli*. *Microbiol Mol Biol Rev* 65:523–569. <https://doi.org/10.1128/MMBR.65.4.523-569.2001>.
- Burlingame R, Chapman PJ. 1983. Catabolism of phenylpropionic acid and its 3-hydroxy derivative by *Escherichia coli*. *J Bacteriol* 155:113–121.
- Xu Y, Gao XL, Wang SH, Liu H, Williams PA, Zhou NY. 2012. MhbT is a specific transporter for 3-hydroxybenzoate uptake by Gram-negative bacteria. *Appl Environ Microbiol* 78:6113–6120. <https://doi.org/10.1128/AEM.01511-12>.
- Xu Y, Wang SH, Chao HJ, Liu SJ, Zhou NY. 2012. Biochemical and molecular characterization of the gentisate transporter GenK in *Corynebacterium glutamicum*. *PLoS One* 7:e38701. <https://doi.org/10.1371/journal.pone.0038701>.
- Dagley S, Chapman PJ, Gibson DT. 1965. The metabolism of *beta*-phenylpropionic acid by an *Achromobacter*. *Biochem J* 97:643–650. <https://doi.org/10.1042/bj0970643>.
- Barnes MR, Duetz WA, Williams PA. 1997. A 3-(3-hydroxyphenyl)propionic acid catabolic pathway in *Rhodococcus globerulus* PWD1: cloning and characterization of the *hpp* operon. *J Bacteriol* 179:6145–6153. <https://doi.org/10.1128/jb.179.19.6145-6153.1997>.
- Arai H, Yamamoto T, Ohishi T, Shimizu T, Nakata T, Kudo T. 1999. Genetic organization and characteristics of the 3-(3-hydroxyphenyl)propionic acid degradation pathway of *Comamonas testosteroni* TA441. *Microbiol-SGM* 145:2813–2820. <https://doi.org/10.1099/00221287-145-10-2813>.
- Pérez-Pantoja D, De la Iglesia R, Pieper DH, González B. 2008. Metabolic reconstruction of aromatic compounds degradation from the genome of the amazing pollutant-degrading bacterium *Cupriavidus necator* JMP134. *FEMS Microbiol Rev* 32:736–794. <https://doi.org/10.1111/j.1574-6976.2008.00122.x>.
- Burlingame RP, Wyman L, Chapman PJ. 1986. Isolation and characterization of *Escherichia coli* mutants defective for phenylpropionate degradation. *J Bacteriol* 168:55–64. <https://doi.org/10.1128/jb.168.1.55-64.1986>.
- Park M, Jeon Y, Jang HH, Ro HS, Park W, Madsen EL, Jeon CO. 2007. Molecular and biochemical characterization of 3-hydroxybenzoate 6-hydroxylase from *Polaromonas naphthalenivorans* CJ2. *Appl Environ Microbiol* 73:5146–5152. <https://doi.org/10.1128/AEM.00782-07>.
- Gao X, Tan CL, Yeo CC, Poh CL. 2005. Molecular and biochemical characterization of the *xlnD*-encoded 3-hydroxybenzoate 6-hydroxylase involved in the degradation of 2,5-xylene via the gentisate pathway in *Pseudomonas alcaligenes* NCIMB 9867. *J Bacteriol* 187:7696–7702. <https://doi.org/10.1128/JB.187.22.7696-7702.2005>.
- Liu TT, Xu Y, Liu H, Luo S, Yin YJ, Liu SJ, Zhou NY. 2011. Functional characterization of a gene cluster involved in gentisate catabolism in *Rhodococcus* sp. strain NCIMB 12038. *Appl Microbiol Biotechnol* 90:671–678. <https://doi.org/10.1007/s00253-010-3033-1>.
- Hiroto T, Fujiwara S, Hosokawa K, Yamaguchi H. 2006. Crystal structure of 3-hydroxybenzoate hydroxylase from *Comamonas testosteroni* has a large tunnel for substrate and oxygen access to the active site. *J Mol Biol* 364:878–896. <https://doi.org/10.1016/j.jmb.2006.09.031>.
- Michalover JL, Ribbons DW, Hughes H. 1973. 3-Hydroxybenzoate 4-hydroxylase from *Pseudomonas testosteroni*. *Biochem Biophys Res Commun* 55:888–896. [https://doi.org/10.1016/0006-291x\(73\)91227-8](https://doi.org/10.1016/0006-291x(73)91227-8).
- Premkumar R, Rao PV, Sreeleela NS, Vaidyanathan CS. 1969. *m*-Hydroxybenzoic acid 4-hydroxylase from *Aspergillus niger*. *Can J Biochem* 47:825–827. <https://doi.org/10.1139/o69-129>.
- Cooper RA, Skinner MA. 1980. Catabolism of 3- and 4-hydroxyphenylacetate by the 3,4-dihydroxyphenylacetate pathway in *Escherichia coli*. *J Bacteriol* 143:302–306.
- Van Berkel WJ, Van Den Tweel WJ. 1991. Purification and characterization of 3-hydroxyphenylacetate 6-hydroxylase: a novel FAD-dependent monooxygenase from a *Flavobacterium* species. *Eur J Biochem* 201:585–592. <https://doi.org/10.1111/j.1432-1033.1991.tb16318.x>.
- Ferrer-Sevillano F, Fernández-Cañón JM. 2007. Novel *phacB*-encoded cytochrome P450 monooxygenase from *Aspergillus nidulans* with 3-hydroxyphenylacetate 6-hydroxylase and 3,4-dihydroxyphenylacetate 6-hydroxylase activities. *Eukaryot Cell* 6:514–520. <https://doi.org/10.1128/EC.00226-06>.
- Ferrandez A, Garcia JL, Diaz E. 1997. Genetic characterization and expression in heterologous hosts of the 3-(3-hydroxyphenyl)propionate catabolic pathway of *Escherichia coli* K-12. *J Bacteriol* 179:2573–2581. <https://doi.org/10.1128/jb.179.8.2573-2581.1997>.
- Spence EL, Kawamukai M, Sanvoisin J, Braven H, Bugg T. 1996. Catechol dioxygenases from *Escherichia coli* (MhpB) and *Alcaligenes eutrophus* (MpcI): sequence analysis and biochemical properties of a third family of extradiol dioxygenases. *J Bacteriol* 178:5249–5256. <https://doi.org/10.1128/jb.178.17.5249-5256.1996>.
- Torres B, Porras G, Garcia JL, Diaz E. 2003. Regulation of the *mhp* cluster responsible for 3-(3-hydroxyphenyl)propionic acid degradation in *Escherichia coli*. *J Biol Chem* 278:27575–27585. <https://doi.org/10.1074/jbc.M303245200>.
- Poehlein A, Kusian B, Friedrich B, Daniel R, Bowien B. 2011. Complete genome sequence of the type strain *Cupriavidus necator* N-1. *J Bacteriol* 193:5017. <https://doi.org/10.1128/JB.05660-11>.
- Vollmers J, Voget S, Dietrich S, Gollnow K, Smits M, Meyer K, Brinkhoff T, Simon M, Daniel R. 2013. Poles apart: Arctic and Antarctic *Octadecabacter* strains share high genome plasticity and a new type of xanthorhodopsin. *PLoS One* 8:e63422. <https://doi.org/10.1371/journal.pone.0063422>.
- Bialek-Davenet S, Criscuolo A, Ailloud F, Passet V, Jones L, Delannoy-Vieillard A-S, Garin B, Le Hello S, Arlet G, Nicolas-Chanoine M-H, Decré D, Brisse S. 2014. Genomic definition of hypervirulent and multidrug-resistant *Klebsiella pneumoniae* clonal groups. *Emerg Infect Dis* 20:1812–1820. <https://doi.org/10.3201/eid2011.140206>.
- Sonnenschein EC, Phippen CBW, Nielsen KF, Mateiu RV, Melchiorson J, Gram L, Overmann J, Freese HM. 2017. *Phaeobacter piscinae* sp. nov., a species of the *Roseobacter* group and potential aquaculture probiont. *Int J Syst Evol Microbiol* 67:4559–4564. <https://doi.org/10.1099/ijsem.0.002331>.
- Yang YF, Zhang JJ, Wang SH, Zhou NY. 2010. Purification and characterization of the *nagl2923*-encoded 3-hydroxybenzoate 6-hydroxylase from *Corynebacterium glutamicum*. *J Basic Microbiol* 50:599–604. <https://doi.org/10.1002/jobm.201000053>.
- Shen XH, Jiang CY, Huang Y, Liu ZP, Liu SJ. 2005. Functional identification of novel genes involved in the glutathione-independent gentisate pathway in *Corynebacterium glutamicum*. *Appl Environ Microbiol* 71:3442–3452. <https://doi.org/10.1128/AEM.71.7.3442-3452.2005>.
- Miramar MD, Costantini P, Ravagnan L, Saraiva LM, Haouzi D, Brothers G, Penninger JM, Peleato ML, Kroemer G, Susin SA. 2001. NADH oxidase activity of mitochondrial apoptosis-inducing factor. *J Biol Chem* 276:16391–16398. <https://doi.org/10.1074/jbc.M010498200>.
- Xiao Y, Liu TT, Dai H, Zhang JJ, Liu H, Tang H, Leak DJ, Zhou NY. 2012. OnpA, an unusual flavin-dependent monooxygenase containing a cytochrome *b₅* domain. *J Bacteriol* 194:1342–1349. <https://doi.org/10.1128/JB.06411-11>.
- Orser CS, Lange CC, Xun L, Zahrt TC, Schneider BJ. 1993. Cloning, sequence analysis, and expression of the *Flavobacterium* pentachlorophenol-4-monooxygenase gene in *Escherichia coli*. *J Bacteriol* 175:411–416. <https://doi.org/10.1128/jb.175.2.411-416.1993>.
- Cai M, Xun L. 2002. Organization and regulation of pentachlorophenol-degrading genes in *Sphingobium chlorophanicum* ATCC 39723. *J Bacteriol* 184:4672–4680. <https://doi.org/10.1128/jb.184.17.4672-4680.2002>.
- Trefault N, De la Iglesia R, Molina AM, Manzano M, Ledger T, Pérez-Pantoja D, Sánchez MA, Stuardo M, González B. 2004. Genetic organization of the catabolic plasmid pJP4 from *Ralstonia eutropha* JMP134

- (pJP4) reveals mechanisms of adaptation to chloroaromatic pollutants and evolution of specialized chloroaromatic degradation pathways. *Environ Microbiol* 6:655–668. <https://doi.org/10.1111/j.1462-2920.2004.00596.x>.
34. Louie TM, Webster CM, Xun L. 2002. Genetic and biochemical characterization of a 2,4,6-trichlorophenol degradation pathway in *Ralstonia eutropha* JMP134. *J Bacteriol* 184:3492–3500. <https://doi.org/10.1128/JB.184.13.3492-3500.2002>.
 35. Kitagawa W, Kimura N, Kamagata Y. 2004. A novel *p*-nitrophenol degradation gene cluster from a Gram-positive bacterium, *Rhodococcus opacus* SAO101. *J Bacteriol* 186:4894–4902. <https://doi.org/10.1128/JB.186.15.4894-4902.2004>.
 36. Hubner A, Danganan CE, Xun L, Chakrabarty AM, Hendrickson W. 1998. Genes for 2,4,5-trichlorophenoxyacetic acid metabolism in *Burkholderia cepacia* AC1100: characterization of the *tftC* and *tftD* genes and locations of the *tft* operons on multiple replicons. *Appl Environ Microbiol* 64:2086–2093.
 37. Nelson WC, Maezato Y, Wu YW, Romine MF, Lindemann SR. 2016. Identification and resolution of microdiversity through metagenomic sequencing of parallel consortia. *Appl Environ Microbiol* 82:255–267. <https://doi.org/10.1128/AEM.02274-15>.
 38. Arias-Barrau E, Sandoval A, Naharro G, Olivera ER, Luengo JM. 2005. A two-component hydroxylase involved in the assimilation of 3-hydroxyphenyl acetate in *Pseudomonas putida*. *J Biol Chem* 280:26435–26447. <https://doi.org/10.1074/jbc.M501988200>.
 39. Bailey LJ, Acheson JF, McCoy JG, Elsen NL, Phillips GN, Jr, Fox BG. 2012. Crystallographic analysis of active site contributions to regioselectivity in the diiron enzyme toluene 4-monooxygenase. *Biochemistry* 51:1101–1113. <https://doi.org/10.1021/bi2018333>.
 40. Chen R, Oki H, Scott RP, Jr, Yamaguchi H, Kusunoki M, Matsuura Y, Chaen H, Tsugita A, Hosokawa K. 1998. Crystallization and future characterization of *meta*-hydroxybenzoate 4-hydroxylase from *Comamonas testoteroni*. *Res Commun Biochem Cell Mol Biol* 2:253–274.
 41. Lountos GT, Mitchell KH, Studts JM, Fox BG, Orville AM. 2005. Crystal structures and functional studies of T4moD, the toluene 4-monooxygenase catalytic effector protein. *Biochemistry* 44:7131–7142. <https://doi.org/10.1021/bi047459g>.
 42. Chen Q, Huang Y, Duan Y, Li Z, Cui Z, Liu W. 2018. Crystal structure of *p*-nitrophenol 4-monooxygenase PnpA from *Pseudomonas putida* DLL-E4: the key enzyme involved in *p*-nitrophenol degradation. *Biochem Biophys Res Commun* 504:715–720. <https://doi.org/10.1016/j.bbrc.2018.09.040>.
 43. Kanteev M, Bregman-Cohen A, Deri B, Shahar A, Adir N, Fishman A. 2015. A crystal structure of 2-hydroxybiphenyl 3-monooxygenase with bound substrate provides insights into the enzymatic mechanism. *Biochim Biophys Acta* 1854:1906–1913. <https://doi.org/10.1016/j.bbapap.2015.08.002>.
 44. Bertani G. 1951. Studies on lysogeny. I. The mode of phage liberation by lysogenic *Escherichia coli*. *J Bacteriol* 62:293–300.
 45. Bertani G. 2004. Lysogeny at mid-twentieth century: P1, P2, and other experimental systems. *J Bacteriol* 186:595–600. <https://doi.org/10.1128/jb.186.3.595-600.2004>.
 46. Sambrook J, Fritsch EF, Maniatis T. 1989. *Molecular cloning: a laboratory manual*, 2nd ed. Cold Spring Harbor Laboratory Press, Cold Spring Harbor, NY.
 47. Datsenko KA, Wanner BL. 2000. One-step inactivation of chromosomal genes in *Escherichia coli* K-12 using PCR products. *Proc Natl Acad Sci U S A* 97:6640–6645. <https://doi.org/10.1073/pnas.120163297>.
 48. Bachmann BJ. 1972. Pedigrees of some mutant strains of *Escherichia coli* K-12. *Bacteriol Rev* 36:525–557.
 49. Zwietering MH, Jongenburger I, Rombouts FM, van't Riet K. 1990. Modeling of the bacterial growth curve. *Appl Environ Microbiol* 56:1875–1881.
 50. Zhou NY, Fuenmayor SL, Williams PA. 2001. *nag* genes of *Ralstonia* (formerly *Pseudomonas*) sp. strain U2 encoding enzymes for gentisate catabolism. *J Bacteriol* 183:700–708. <https://doi.org/10.1128/JB.183.2.700-708.2001>.
 51. Zhao H, Xu Y, Lin S, Spain JC, Zhou NY. 2018. The molecular basis for the intramolecular migration (NIH shift) of the carboxyl group during *para*-hydroxybenzoate catabolism. *Mol Microbiol* 110:411–424. <https://doi.org/10.1111/mmi.14094>.
 52. de Lorenzo V, Eltis L, Kessler B, Timmis KN. 1993. Analysis of *Pseudomonas* gene products using *lacI^q/Ptrp-lac* plasmids and transposons that confer conditional phenotypes. *Gene* 123:17–24. [https://doi.org/10.1016/0378-1119\(93\)90533-9](https://doi.org/10.1016/0378-1119(93)90533-9).